

Attenuation-based Automatic Tube Voltage Selection and Tube Current Modulation for Dose Reduction at Contrast-enhanced Liver CT¹

Kyung Hee Lee, MD
Jeong Min Lee, MD
Sung Kyoung Moon, MD
Jee Hyun Baek, MD
Ji Hoon Park, MD
Thomas G. Flohr, PhD
Kyung Won Kim, MD
Soo Jin Kim, MD
Joon Koo Han, MD
Byung Ihn Choi, MD

Purpose:

To retrospectively determine whether the combined use of automatic tube voltage selection (ATVS) and automatic tube current modulation (ATCM) can effectively reduce radiation dose at contrast material-enhanced liver computed tomography (CT) while maintaining acceptable image quality compared with the use of ATCM alone.

Materials and Methods:

This study was approved by an institutional review board, and informed consent was waived. Three hundred fourteen consecutive patients suspected of having liver disease were divided into three groups. In two groups, both ATVS and ATCM were used (group A1, $n = 97$; group A2, $n = 101$) but with different contrast gain settings; in one group, only ATCM with a fixed tube potential of 120 kV (group B, $n = 116$) was used. Weighted volume CT dose index and dose-length product, contrast-to-noise ratios (CNRs), and mean image noise were assessed. Qualitative analysis was performed by two board-certified radiologists and one radiology resident. Statistical analysis was performed by using the one-way analysis of variance test, two-tailed paired t test, Kruskal-Wallis test, and noninferiority test.

Results:

In groups A1 and A2, a significant dose reduction was obtained compared with that in group B ($P < .0001$). The mean dose reduction was 20% in group A1 and 31% in group A2. Furthermore, CNRs were significantly higher in groups A1 and A2 than in group B ($P < .0001$). Despite the higher image noise in groups A1 and A2, the overall image quality was acceptable.

Conclusion:

Compared with the use of ATCM alone, the combined use of ATVS and ATCM allowed reduction of radiation exposure while maintaining good image quality at contrast-enhanced liver CT.

©RSNA, 2012

Supplemental material: <http://radiology.rsna.org/lookup/suppl/doi:10.1148/radiol.12112434/-/DC1>

¹From the Division of Abdominal Imaging, Department of Radiology, Institute of Radiation Medicine, Seoul National University College of Medicine, 28 Yeongon-dong, Jongno-gu, Seoul 110-744, Korea (K.H.L., J.M.L., S.K.M., J.H.B., J.H.P., K.W.K., S.J.K., J.K.H., B.I.C.); and Siemens Medical Solutions, Forchheim, Germany (T.G.F.). From the 2011 RSNA Annual Meeting. Received November 21, 2011; revision requested January 27, 2012; revision received April 2; accepted April 24; final version accepted May 10. Address correspondence to J.M.L. (e-mail: jmsh@snu.ac.kr).

The use of diagnostic computed tomographic (CT) imaging has increased remarkably during the past 2 decades owing to technologic developments, its increasing availability, and the perception that imaging can play an important role in the detection and staging of disease, as well as in helping to make medical decisions (1). However, concerns have also been raised regarding potential patient health risks due to radiation exposure (2,3). With radiation dose reduction having become a critical issue, various techniques and patient-based dose modulations have been developed to optimize and reduce radiation dose during CT examinations, including x-ray beam collimation, filtration, automatic tube current modulation (ATCM), and lower tube voltage (4–8). The general principle for dose management at CT has been that the examination must be medically indicated (justification) and performed by using doses that are as low as reasonably achievable (or ALARA) and consistent with the diagnostic task (9–11).

Among the various dose-reduction techniques, ATCM, which enables automatic adjustment of tube current based on size and attenuation characteristics of the body part being scanned, has been the most frequently used method for dose reduction. Still, other considerations, such as adjusting tube voltage on the basis of patient size or iterative reconstruction techniques, have been proposed, which also result in further dose reduction (11–18). Several CT phantom studies have

suggested that tube voltage settings should reflect the diagnostic purpose of the CT examination as well as the patient's body size (14,19). In addition, several clinical studies have reported the utility of the low tube voltage technique for CT angiography, for abdominal CT examinations, and in pediatric patients (12,20–22). A particularly interesting study was the experimental phantom study performed by Yu et al (14), which demonstrated the feasibility of a new strategy allowing automatic tube voltage selection (ATVS) based on the patient's body habitus and the specific diagnostic task at hand. On the basis of the core principles of ATVS, which was demonstrated by Yu et al (14), a new commercially available software (Care kV; Siemens Healthcare, Forchheim, Germany) that allows the simultaneous use of ATVS and ATCM has recently been developed. However, instead of using noise constraint as an image quality index as proposed by Yu et al (14), the ATVS program (Care kV) utilizes contrast-to-noise ratio (CNR) as the image quality index. To date, this intriguing concept of ATVS has only been tested in one clinical report for CT angiography (23).

Therefore, the purpose of our study was to determine whether the combined use of ATVS and ATCM can effectively reduce radiation dose at contrast material-enhanced liver CT while maintaining acceptable image quality compared with the use of ATCM alone.

Materials and Methods

This study was approved by the institutional review board at Seoul National University Hospital, and the

Implication for Patient Care

- The combined use of ATVS and ATCM techniques can be a more effective strategy for reducing patient radiation dose while attaining acceptable image quality during multidetector liver CT examinations than the use of ATCM alone with a fixed tube potential of 120 kV.

requirement for written informed consent was waived for all patients in this retrospective study. Because a Siemens ATVS program was evaluated in this study and one author (T.G.F.) is an employee of Siemens Healthcare (Chicago, Ill), full control of the data and information presented for publication was maintained by those authors (J.M.L., K.H.L.) who are not employees of Siemens Healthcare.

Patient Population

For this retrospective study, we collected consecutive patient data during the initial Care kV setup period from June to August 2010. Care kV had first been utilized for liver CT in clinical practice at our institution in June 2010. In total, 330 consecutive patients who had undergone quadruple-phase liver CT with a CT scanner (Somatom Definition Dual Source; Siemens Medical Solutions, Forchheim, Germany) were identified. Sixteen of these patients were later excluded from the study because (a) a different reconstruction algorithm (iterative reconstruction in image space) other than B30 filtered back projection had been used ($n = 15$) or

Advance in Knowledge

- With the combined use of automatic tube voltage selection (ATVS) and automatic tube current modulation (ATCM), a 20%–31% dose reduction in volume CT dose index and dose-length product ($P < .0001$) was achieved without compromising image quality compared with the use of ATCM alone with a fixed tube potential of 120 kV at liver CT.

Published online before print

10.1148/radiol.12112434 Content codes: **GI** **CT**

Radiology 2012; 265:437–447

Abbreviations:

AP = arterial phase
 ATCM = automatic tube current modulation
 ATVS = automatic tube voltage selection
 BMI = body mass index
 CNR = contrast-to-noise ratio
 CTDI_{vol} = volume CT dose index
 DP = delayed phase
 PVP = portal venous phase

Author contributions:

Guarantors of integrity of entire study, K.H.L., J.M.L.; study concepts/study design or data acquisition or data analysis/interpretation, all authors; manuscript drafting or manuscript revision for important intellectual content, all authors; manuscript final version approval, all authors; literature research, K.H.L., J.M.L., S.J.K., J.K.H., B.I.C.; clinical studies, K.H.L., J.M.L., S.K.M., J.H.B., J.H.P., K.W.K., S.J.K.; statistical analysis, K.H.L.; and manuscript editing, K.H.L., J.M.L., J.H.B., J.H.P., T.G.F.

Conflicts of interest are listed at the end of this article.

(b) body weight and height data were not available ($n = 1$). The remaining 314 patients (mean age, 59.7 years; age range, 23–87 years; 226 men [mean age, 59.4 years; age range, 23–86 years], 88 women [mean age, 60.5 years; age range, 28–87 years]) were divided into three groups on the basis of the study period and protocol used and ultimately comprised our study population. In the first third of the study period, 97 patients underwent CT scanning by using the Care kV program with the eighth ATVS setting (group A1). In the middle third of the study period, 101 patients underwent CT examination by using the Care kV program with the 10th ATVS setting (group A2). The remaining 116 patients underwent CT scanning by using the standard protocol of ATCM only with a fixed tube potential of 120 kV in the last third of the study period (group B). As we utilized patient data of the initial protocol setup period, reverting to ATCM with a fixed tube potential was done to allow sufficient time to review the images obtained from ATVS and ATCM and then to determine the contrast gain factor.

No significant differences in age ($P = .37$, one-way analysis of variance test), body mass index (BMI) distribution ($P = .72$, one-way analysis of variance test), or sex ($P = .32$, χ^2 test) were observed among the three patient groups. In addition, the presence of underlying disease (ie, chronic liver disease or liver cirrhosis) and the distribution of Child-Pugh score did not differ significantly among the three groups ($P = .84$ and $.78$, respectively, χ^2 test).

Principle of ATVS Program

The ATVS program (Care kV) is designed to automatically recommend the tube voltage setting that provides the lowest radiation dose among four tube voltage settings (80, 100, 120, and 140 kV) for each individual patient dependent on the diagnostic task to be performed. To ensure equivalence in image quality, Care kV pays close attention to matching the CNR at each tube voltage on the basis of the concept of “contrast gain,” defined as the ratio of iodine

versus water or soft-tissue attenuation difference at a given tube voltage relative to that at 140 kV, considered a reference of 1. More specific details on this program are provided in Appendix E1 (online). This program was designed to work in conjunction with ATCM (CARE Dose 4D; Siemens Medical Solutions), which modulates tube current on the basis of the patient’s geometry and anatomy after the optimal tube voltage is selected by Care kV.

To initiate ATVS, users must first select one appropriate setting from 12 settings on the basis of the diagnostic purpose of the CT examination. Diagnostic purpose means more or less the relevance of iodine contrast in a trade-off between image noise and contrast enhancement in our study (Table 1). For the purposes of liver CT in this study, two ATVS gain settings (eighth and 10th ATVS settings in Table 1) were used on the basis of the theoretical estimation of the most appropriate setting and the vendor’s recommendations (Appendix E1 [online]). For the tube voltage selection process of the Care kV program, CT projection radiographs (“topograms”) for each patient were used to analyze each patient’s size and attenuation characteristics. Once the diagnostic task was determined, patient-specific tube current curves were calculated for all tube voltage levels (Fig E1 [online]) necessary to deliver the desired image quality on the basis of the selected scan range on the patient’s topogram. The program then calculated the estimated radiation dose on the basis of these tube voltage-specific tube current curves for all of the tube voltage levels to determine the optimal dose efficiency. Once the optimal settings were determined, the tool took into account scanner limitations such as maximum tube current or restrictions due to limited heat capacity. If the selected setting was not possible because of the previously stated limitations, the next best tube voltage setting was suggested.

CT Protocol

For all patients, quadruple-phase CT consisting of precontrast, arterial phase (AP), portal venous phase (PVP), and

delayed phase (DP) imaging was performed. In groups A1 and A2, the combined use of ATVS and ATCM was applied for AP and PVP images, while ATCM with a fixed tube potential of 120 kV was used for precontrast and DP images. In group B, ATCM with a fixed tube potential of 120 kV was used for all four phases. For five patients in group A1 and 15 patients in group A2, automatic tube potential was selected only for AP images. Data from these patients were excluded in the evaluation of PVP images. All patients underwent scanning (Somatom Definition Dual Source CT [DSCT]; Siemens Medical Solutions) in the single-energy mode. CT parameters are described in detail in Table 2.

Radiation Dose

The volume CT dose index ($CTDI_{vol}$) and dose-length product on AP and DP images were obtained for each patient. Radiation dose reduction (in percentages) was calculated on the basis of the $CTDI_{vol}$ and dose-length product during the AP (combined use of ATVS and ATCM) divided by the $CTDI_{vol}$ and dose-length product during the DP (ATCM with fixed 120 kV).

BMI Group Analysis

To analyze radiation dose reduction according to patient sizes, patients were categorized into five groups according to their BMI (less than 18.5 kg/m², underweight; between 18.5 and 22.9 kg/m², normal; between 23 and 24.9 kg/m², overweight; between 25 and 29.9 kg/m², obese; and 30 kg/m² or greater, severely obese) (24). On the basis of these five BMI groups, the recommended tube potentials were analyzed in groups A1 and A2.

Image Analysis

Quantitative analysis.—A single radiologist (K.H.L., with 4 years of clinical experience), who was not involved in the qualitative analysis, measured the image noise and enhancement of the liver, abdominal aorta, portal vein, and paraspinal muscle, as described in previous reports (13,25) (Appendix E2 [online]). CNRs relative to muscle for the organ of interest were calculated by using the following equation

(26): $CNR_o = (ROI_o - ROI_m)/SD_n$, where ROI_o is the mean attenuation of the organ at interest, ROI_m is the mean attenuation of the paraspinal muscle, and SD_n is the mean image noise.

Qualitative analysis.—Two attending abdominal radiologists (J.H.B. [observer 1] and S.K.M. [observer 2] with 7 and 6 years of clinical experience, respectively) and one radiology chief resident (J.H.P. [observer 3]) independently analyzed the AP and PVP liver CT images at the same picture archiving and communication system workstation (Maroview; Marotech, Seoul, Korea) on a 5-megapixel liquid crystal display monitor. The reading order of the 314 liver CT studies was randomized. For blind evaluation, images presented to the radiologists did not include patient demographics or CT parameters. Although the images were initially presented on a preset soft-tissue window (window width, 350 HU; window level, 40 HU), the readers were allowed to adjust the window setting at their discretion. The three readers were asked to rank the quality of the images on the basis of a previously reported three-point or five-point scoring scheme (Appendix E3 [online]) (4,20,27). The assessment of image noise, overall image quality, and visibility of small vascular structures was according to a five-point scale, while the evaluation of beam-hardening artifacts and abdominal-organ enhancement was done by using a three-point scale. On both AP and PVP images, image noise, beam-hardening artifacts, and overall image quality were assessed. Furthermore, visibility of small vascular structures was evaluated on AP images, and abdominal-organ contrast enhancement was evaluated on PVP images.

Lesion Analysis: Hypervascular Hepatocellular Carcinomas

Among the 314 patients, 35 (group A1, $n = 10$; group A2, $n = 12$; group B, $n = 13$) had solitary or multiple hypervascular hepatocellular carcinoma nodules. In total, 46 hypervascular tumors (group A1, $n = 15$; group A2, $n = 12$; group B, $n = 19$) were identified in 35 patients. Proof of hepatocellular carcinoma was not obtained

Table 1

Contrast Gain of Each Tube Voltage at ATVS Settings of the Care kV Program in Groups A1 and A2

| ATVS Setting | 80 kV | 100 kV | 120 kV | 140 kV | Comment |
|--------------|-------|--------|--------|--------|--|
| 1 | 1.000 | 1.000 | 1.000 | 1.000 | No contrast gain, equal noise |
| 2 | 1.089 | 1.045 | 1.018 | 1.000 | |
| 3 | 1.178 | 1.089 | 1.036 | 1.000 | |
| 4 | 1.267 | 1.134 | 1.055 | 1.000 | |
| 5 | 1.356 | 1.178 | 1.073 | 1.000 | |
| 6 | 1.446 | 1.223 | 1.091 | 1.000 | |
| 7 | 1.535 | 1.267 | 1.109 | 1.000 | |
| 8 | 1.624 | 1.312 | 1.127 | 1.000 | Group A1 |
| 9 | 1.713 | 1.356 | 1.146 | 1.000 | |
| 10 | 1.802 | 1.401 | 1.164 | 1.000 | Group A2 |
| 11 | 1.891 | 1.446 | 1.182 | 1.000 | |
| 12 | 1.980 | 1.490 | 1.200 | 1.000 | Maximum contrast gain, highest image noise |

Note.—All numbers stand for the contrast gain at the given tube voltage, defined as the relative ratio of iodine versus water or soft-tissue attenuation difference at a given tube voltage relative to that at 140 kV, considered a reference of 1 at contrast-enhanced CT. From ATVS settings 1 to 12, “quality of reference tube current” for each tube potential is modified, and in each row, the same image quality in terms of iodine CNR is maintained in all tube voltages. The ATVS setting 1 is the reference setting without any contrast material, in which equal noise and equal radiation dose is obtained along all four tube voltages; ATVS setting 12 makes maximum use of iodine contrast gain at lower tube voltages (iodine contrast gain 1.980 when going from 140 kV to 80 kV) and allows the highest image noise at lower tube voltage. The ATVS setting from 2 to 11 represents contrast gain values that are mainly linear interpolations from ATVS setting 1 to ATVS setting 12. In this study, two different ATVS settings were applied for groups A1 and A2 (contrast gain of 1.624 and 1.802, respectively, when going from 140 to 80 kV).

Table 2

CT Scanning Parameters

| Parameter | Datum |
|---|---|
| Detector configuration* | 64 × 0.625 |
| Gantry rotation time (sec) | 0.5 |
| Pitch | 0.8–1.0 |
| Acquisition mode | Axial |
| Reconstructed section thickness (mm) | 3 |
| Field of view (cm) | 36 |
| Reconstruction kernel | Standard |
| Contrast medium | Iopromide (Ultravist 370; Schering, Berlin, Germany) |
| Iodine concentration (milligram of iodine per milliliter) | 370 |
| Total amount (milliliter per kilogram of body weight) | 1.5 |
| Injection rate (mL/sec) | 2.0–4.0 |
| Scan delay after start of injection | AP, 19 sec after 100 HU of the descending aorta as measured by using the bolus-tracking technique; PVP, 33 sec; DP, 180 sec |

* Value for collimation refers to number of sections × section thickness in millimeters.

with histopathologic findings, but with typical imaging findings of hypervascular mass larger than 1 cm in diameter, which showed washout on venous phase images (28). In cases with three

or more tumors, only the three largest tumors were included.

For quantitative lesion analysis, one radiologist (K.H.L.), who was not made aware of the CT protocol used,

Table 3

Recommended Tube Potentials and Their Radiation Dose of the Three Groups

| Parameter | Group A1 | Group A2 | Group B | PValue* | PValue† | | |
|---------------------------------------|-----------|-----------|-----------|---------|----------|---------|---------|
| | | | | | A1 vs A2 | A1 vs B | A2 vs B |
| Tube voltage (kV)‡ | | | | | | | |
| 80 | 43 (44.3) | 64 (63.4) | 0 (0) | ... | ... | ... | ... |
| 100 | 53 (54.6) | 34 (33.7) | 0 (0) | ... | ... | ... | ... |
| 120 | 0 (0) | 0 (0) | 116 (100) | ... | ... | ... | ... |
| 140 | 1 (1.1) | 3 (2.9) | 0 (0) | ... | ... | ... | ... |
| CTDI_{vol} (mGy) | | | | | | | |
| AP | 7.7 ± 2.2 | 6.9 ± 3.3 | 9.4 ± 1.8 | <.0001 | .06 | <.0001 | <.0001 |
| PVP | 7.7 ± 2.2 | 6.9 ± 3.4 | 9.4 ± 1.8 | <.0001 | .11 | <.0001 | <.0001 |
| DP | 9.4 ± 1.6 | 9.6 ± 2.3 | 9.4 ± 1.8 | .63 | ... | ... | ... |
| Dose-length product (mGy · cm) | | | | | | | |
| AP | 179 ± 61 | 162 ± 82 | 220 ± 53 | <.0001 | .17 | <.0001 | <.0001 |
| PVP | 180 ± 59 | 164 ± 87 | 220 ± 54 | <.0001 | .24 | <.0001 | <.0001 |
| DP | 220 ± 48 | 225 ± 64 | 220 ± 54 | .76 | ... | ... | ... |
| Dose reduction (%)§ | 20 ± 12.1 | 31 ± 15.9 | 0 ± 1.1 | <.0001 | <.0001 | <.0001 | <.0001 |
| Dose reduction (%) | 20 ± 13.0 | 31 ± 15.9 | 0 ± 1.8 | <.0001 | <.0001 | <.0001 | <.0001 |

Note.—Unless otherwise specified, data are means ± standard deviations.

* Calculated by using one-way analysis of variance.

† Calculated by using Tukey posthoc comparison tests.

‡ Data are numbers of patients, with the percentages in parentheses.

§ Dose reduction (%) = (CTDI_{vol} of DP – CTDI_{vol} of AP)/CTDI_{vol} of DP × 100.

|| Dose reduction (%) = (DLP of DP – DLP of AP)/DLP of DP × 100, where DLP is dose-length product.

measured the attenuation of the most enhanced portion of the tumor. An attempt was made to maintain a region of interest of 50 mm². The attenuation of adjacent normal liver parenchyma was also measured in an approximate region of interest of 200 mm². The tumor-to-liver contrast then was calculated as the attenuation difference between the hypervascular tumor and liver parenchyma (25). The tumor-to-liver contrast was measured and averaged in all lesions in cases with fewer than three tumors. In cases with three or more lesions, the tumor-to-liver contrast was measured and averaged in the three largest tumors.

Finally, three readers who participated in the qualitative analysis assessed the conspicuity of 50 hypervascular liver tumors, which were annotated with arrows on AP images. Lesion conspicuity was defined as distinguishability from the liver and was evaluated with a five-point scale (score of 1, not distinct; 2, barely distinct; 3, moderately distinct; 4, fairly distinct; 5, definitely distinct) (29,30).

Statistical Analysis

Continuous variables were reported as means ± standard errors of the mean, and categorical variables were reported in frequencies or percentages. The two-tailed paired *t* test was used for intra-individual comparison of the radiation dose during the arterial scan with both ATVS and ATCM and the delayed scan with 120 kV and ATCM. In addition, the one-way analysis of variance test was used for intergroup comparison of radiation dose and quantitative measurement data. Noninferiority analysis was performed to verify the hypothesis of “maintaining image quality.” The noninferiority of the ATVS program over that of fixed tube potential (120 kV) was established if the lower limit for the 97.5% confidence interval for the difference was greater than –0.2 (31). Finally, the Kruskal-Wallis test was used to determine the results of qualitative analysis and lesion analysis. When statistically significant differences occurred, single posttest comparisons were performed by using the Mann-Whitney *U* test with

Bonferroni correction for multiple comparisons. Interobserver agreement was measured by using the κ test (28). All statistical analyses were performed by using commercially available software (SPSS, version 17.0; SPSS, Chicago, Ill). For all studies, a difference with a *P* value of less than .05 was considered significant.

Results

Recommended Tube Potentials and Their Radiation Dose

CT examinations for groups A1 and A2 were performed with the recommended tube potential provided by the ATVS program; the recommended radiation doses are shown in Table 3. In group A1, 100 kV (53 [54.6%] of 97) was selected most often, and in group A2, 80 kV (64 [63.4%] of 101) was the most frequently recommended tube potential for dose efficiency. Intraindividual comparison of CTDI_{vol} and dose-length product between the AP and the

DP showed that there was a significant dose reduction with the combined use of ATVS and ATCM in groups A1 and A2 ($P < .0001$). In group A1, the mean $CTDI_{vol}$ was $7.7 \text{ mGy} \pm 2.2$ (standard deviation) for the AP and $9.4 \text{ mGy} \pm 1.6$ for the DP, with a decrease of 20% in group A1 ($P < .0001$), whereas in group A2, the values were $6.9 \text{ mGy} \pm 3.3$ for the AP and $9.6 \text{ mGy} \pm 2.3$ for the DP, with a decrease of 31% in group A2. Therefore, dose reduction (in percentages) was greater in group A2 than in group A1 ($P < .0001$). In addition, in the intergroup analysis among the three groups by using the one-way analysis of variance test, the $CTDI_{vol}$ and dose-length product during the AP were significantly lower in groups A1 and A2 than in group B ($P < .0001$).

BMI Group Analysis

Correlation between BMIs and recommended tube potentials in groups A1 and A2 is illustrated in Figure 1. In normal and underweight patients (BMI, $<23 \text{ kg/m}^2$) 80 kV was the most frequently selected dose in groups A1 and A2. In overweight patients (BMI, $23\text{--}24.9 \text{ kg/m}^2$), 100 kV was the most frequent tube potential used in group A1 and 80 kV was that in group A2. In obese patients (BMI, $25\text{--}29.9 \text{ kg/m}^2$), 100 kV was the most commonly used tube potential in groups A1 and A2. In severely obese patients (BMI, 30 kg/m^2 or greater), 140 kV was the most frequent tube potential used in group A2. A dose reduction (mean dose reduction, $20\% \pm 12$ [standard deviation] in group A1; $32\% \pm 15$ in group A2) was obtained in all patients with a BMI of less than 30 kg/m^2 . The mean dose reduction was greatest in underweight patients (33% in group A1 [$n = 1$], $41\% \pm 1$ in group A2 [$n = 5$]), followed by normal-weight patients (27% ± 10 in group A1 [$n = 34$], $40\% \pm 6$ in group A2 [$n = 33$]). However, in severely obese patients, 140 kV was selected, and therefore an increase in the mean radiation dose ($7\% \pm 11$ in group A2 [$n = 4$]) was observed.

Quantitative Image Analysis

Image noise on AP and PVP images was significantly higher in groups A1 and A2

Figure 1

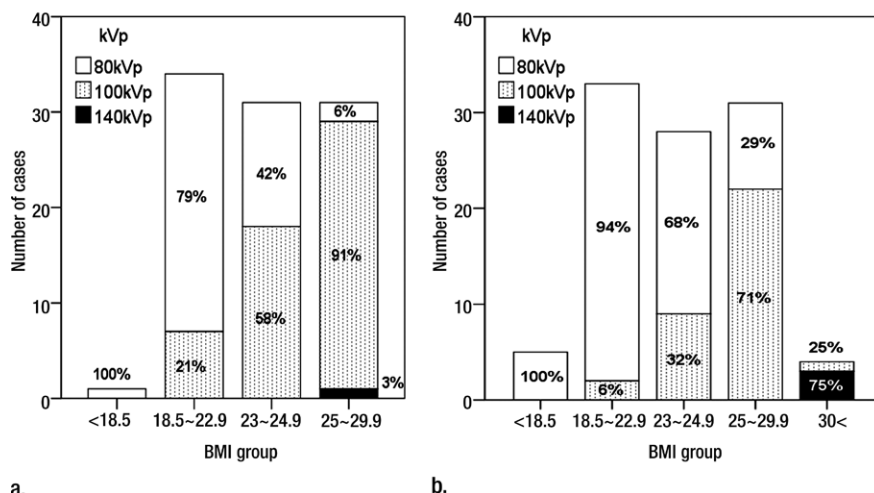


Figure 1: Graphs show distribution of selected tube voltages in patient groups (a) A1 and (b) A2 according to each BMI group.

than in group B: Mean image noise of the AP and PVP images was $11.0 \text{ HU} \pm 0.1$ and $11.2 \text{ HU} \pm 0.1$ in group A1, $12.1 \text{ HU} \pm 0.2$ and $11.9 \text{ HU} \pm 0.2$ in group A2, and $10.3 \text{ HU} \pm 0.1$ and $10.3 \text{ HU} \pm 0.1$ in group B, respectively ($P < .001$). The highest image noise was measured as 18.6 HU on PVP images in a 36-year-old man (body weight, 98 kg; BMI, 32.37 kg/m^2) in group A2, for whom 140 kV was recommended and applied for CT examination.

Comparison of the three groups showed that the mean CT numbers of the aorta and aorta-to-liver on AP images and those of liver, portal vein, and portal vein-to-liver on PVP images were significantly higher in groups A1 and A2 than they were in group B ($P < .0001$) (Table 4). In addition, the CNR of the aorta and CNR of aorta-to-liver on AP images (33.1 ± 0.8 and 32.0 ± 0.8 in group A1; 31.3 ± 0.9 and 30.1 ± 0.9 in group A2; 23.6 ± 0.5 and 22.4 ± 0.5 in group B, respectively) and the CNR of the liver, portal vein, and portal vein-to-liver on PVP images (5.8 ± 0.2 , 15.0 ± 0.4 , and 9.2 ± 0.3 in group A1; 5.6 ± 0.2 , 14.8 ± 0.4 , and 9.2 ± 0.3 in group A2; 4.7 ± 0.2 , 10.4 ± 0.2 , and 5.7 ± 0.2 in group B, respectively) were significantly higher in groups A1 and A2 than in group B ($P < .0001$) (Table 4).

Qualitative Image Analysis

The image quality scores assigned by the three radiologists and the level of inter-observer agreement are shown in Table 5. With regard to the overall image quality, the scores were the highest in group A1 (3.21 on AP, 3.48 on PVP images), followed by group B (3.13 on AP, 3.05 on PVP images) and group A2 (3.06 on AP, 3.26 on PVP images) ($P = .12$ for AP, $P < .0001$ for PVP). The visibility of small hepatic vessels and the abdominal organ enhancement was significantly better in groups A1 (3.73 and 2.71, respectively) and A2 (3.62 and 2.64, respectively) than in group B (3.17 and 2.03, respectively) ($P < .0001$). However, higher image noise ($P < .0001$) and more beam hardening were observed in groups A1 and A2 than in group B ($P < .0001$ for AP, $P = .02$ for PVP): The mean score of image noise on the AP and PVP images was 2.56 and 2.57 in group A1, 2.34 and 2.48 in group A2, and 3.00 and 2.69 in group B, respectively. The mean score of beam hardening on the AP and PVP images was 2.11 and 2.31 in group A1, 2.05 and 2.25 in group A2, and 2.20 and 2.43 in group B, respectively. There were no patients who received an unacceptable score with respect to overall image quality and image noise (Figs 2-4). In groups A1 and A2, the lower limit for the 97.5% confidence interval

Table 4

Quantitative Analysis Results in the Three Patient Groups

| Parameter | Group A1 | Group A2 | Group B | PValue* | PValue† | | |
|----------------------------|-------------|--------------|-------------|---------|----------|---------|---------|
| | | | | | A1 vs A2 | A1 vs B | A2 vs B |
| Noise | | | | | | | |
| AP | 11.0 ± 0.1 | 12.1 ± 0.2 | 10.3 ± 0.1 | <.0001 | <.0001 | <.0001 | <.0001 |
| PVP | 11.2 ± 0.1 | 11.9 ± 0.2 | 10.3 ± 0.1 | <.0001 | .01 | <.0001 | <.0001 |
| CT numbers (HU) | | | | | | | |
| Aorta during AP | 414.6 ± 7.9 | 429.2 ± 10.8 | 291.5 ± 4.1 | <.0001 | .40 | <.0001 | <.0001 |
| Aorta-to-liver during AP | 346.1 ± 7.7 | 359.4 ± 10.6 | 225.8 ± 4.2 | <.0001 | .46 | <.0001 | <.0001 |
| Liver during PVP | 129.5 ± 1.9 | 129.2 ± 2.5 | 107.1 ± 1.4 | <.0001 | .99 | <.0001 | <.0001 |
| Portal vein during PVP | 229.1 ± 4.6 | 231.2 ± 5.2 | 165.3 ± 1.7 | <.0001 | .93 | <.0001 | <.0001 |
| Portal-to-liver during PVP | 100.0 ± 3.4 | 102.0 ± 3.5 | 58.2 ± 1.8 | <.0001 | .83 | <.0001 | <.0001 |
| Muscle during PVP | 66.2 ± 1.1 | 63.6 ± 1.0 | 59.2 ± 0.6 | <.0001 | .12 | <.0001 | .002 |
| CNR | | | | | | | |
| Aorta during AP | 33.1 ± 0.8 | 31.3 ± 0.9 | 23.6 ± 0.5 | <.0001 | .24 | <.0001 | <.0001 |
| Aorta-to-liver during AP | 32.0 ± 0.8 | 30.1 ± 0.9 | 22.4 ± 0.5 | <.0001 | .19 | <.0001 | <.0001 |
| Liver during PVP | 5.8 ± 0.2 | 5.6 ± 0.2 | 4.7 ± 0.2 | <.0001 | .85 | <.0001 | .002 |
| Portal vein during PVP | 15.0 ± 0.4 | 14.8 ± 0.4 | 10.4 ± 0.2 | <.0001 | .95 | <.0001 | <.0001 |
| Portal-to-liver during PVP | 9.2 ± 0.3 | 9.2 ± 0.3 | 5.7 ± 0.2 | <.0001 | >.99 | <.0001 | <.0001 |
| Muscle during PVP | 6.0 ± 0.1 | 5.5 ± 0.1 | 5.8 ± 0.1 | .028 | .03 | .73 | .11 |

Note.—Data are means ± standard errors.

* Calculated by using one-way analysis of variance.

† Calculated by using Tukey post hoc comparison tests.

Table 5

Qualitative Analysis Results in the Three Patient Groups

| Parameter | Group A1 | Group A2 | Group B | Weighted κ | PValue* | PValue† | | |
|-------------------|-------------------|--------------------|--------------------|------------|---------|----------|---------|---------|
| | | | | | | A1 vs A2 | A1 vs B | A2 vs B |
| AP | | | | | | | | |
| Small structures | 3.73 ± 0.8 | 3.62 ± 0.9 | 3.17 ± 0.9 | 0.76 | <.0001 | .53 | <.0001 | <.0001 |
| Image noise | 2.56 ± 0.5 (0/97) | 2.34 ± 0.5 (0/101) | 3.00 ± 0.4 (0/116) | 0.54 | <.0001 | .012 | <.0001 | <.0001 |
| Beam hardening | 2.11 ± 0.3 | 2.05 ± 0.2 | 2.20 ± 0.3 | 0.51 | <.0001 | .12 | .02 | <.0001 |
| Overall quality | 3.21 ± 0.4 (0/97) | 3.06 ± 0.4 (0/101) | 3.13 ± 0.4 (0/116) | 0.44 | .12 | .04 | .22 | .37 |
| PVP | | | | | | | | |
| Organ enhancement | 2.71 ± 0.4 | 2.64 ± 0.5 | 2.03 ± 0.3 | 0.75 | <.0001 | .37 | <.0001 | <.0001 |
| Image noise | 2.57 ± 0.3 (0/92) | 2.48 ± 0.2 (0/86) | 2.69 ± 0.2 (0/116) | 0.40 | <.0001 | .02 | .001 | <.0001 |
| Beam hardening | 2.31 ± 0.4 | 2.25 ± 0.4 | 2.43 ± 0.4 | 0.50 | .02 | .26 | .05 | .003 |
| Overall quality | 3.48 ± 0.5 (0/92) | 3.26 ± 0.5 (0/86) | 3.05 ± 0.3 (0/116) | 0.43 | <.0001 | .006 | <.0001 | <.0001 |

Note.—Data are means ± standard deviations. Data in parentheses are numbers that were rated as unacceptable per numbers of total case. If any of the three readers rated the score of 1 (defined as unacceptable) with a five-point rating scale, the case was rated as unacceptable. For PVP images, five cases in group A1 and 15 cases in group A2 were excluded from qualitative analysis because only AP images were obtained by using both ATVS and ATCM and PVP images were acquired with a fixed tube potential of 120 kV for these patients.

* Calculated by using the Kruskal-Wallis test.

† Calculated by using the Mann-Whitney U test. Bonferroni-corrected P value is .017.

for the difference in overall image score from group B (group A1 or A2 – group B) was greater than –0.2 (–0.044 and –0.195 during AP and 0.260 and 0.068 during PVP in groups A1 and A2,

respectively), and therefore we were able to demonstrate the noninferiority of ATVS over that of fixed tube potential (120 kV). The weighted κ values ranged from 0.4 to 0.76.

Lesion Analysis (Hypervascular Hepatocellular Carcinomas)

For the 46 hypervascular hepatocellular carcinomas in 35 patients, we assessed the tumor-to-liver contrast and lesion

Figure 2



Figure 2: Transverse contrast-enhanced CT images in 42-year-old woman (BMI, 29.14 kg/m²) in group A1. During the (a) AP and (b) PVP, images were obtained with the combined use of ATCM and ATVS at a tube voltage of 100 kV. (c) DP image was obtained with the use of ATCM alone with a fixed tube potential of 120 kV. Window setting was optimized at a window width of 350 HU and a window level of 40 HU for all images. For AP, PVP, and DP images, CTDI_{vol} was 9.34, 9.29, and 10.17 mGy, while the mean image noise was 11.2, 10.5, and 13.2 HU, respectively, measured at the subcutaneous fat of the anterior abdominal wall.

Figure 3



Figure 3: Transverse contrast-enhanced CT images in 72-year-old man (BMI, 27.77 kg/m²) in group A2. During the (a) AP and (b) PVP, images were obtained with the combined use of ATCM and ATVS at a tube voltage of 100 kV. (c) DP image was obtained with the use of ATCM alone with a fixed tube potential of 120 kV. Window setting was optimized at a window width of 350 HU and a window level of 40 HU for all images. For AP, PVP, and DP images, CTDI_{vol} was 8.61, 8.46, and 10.21 mGy, while the mean image noise was 11.8, 11.4, and 13.8 HU, respectively, measured at the subcutaneous fat of the anterior abdominal wall.

conspicuity (Table 6). The tumor-to-liver contrast was significantly higher in groups A1 and A2 than in group B ($P < .0001$). Statistical analysis revealed that there were no significant differences in lesion conspicuity among the three groups.

Discussion

The main findings of this study were that the combined use of ATVS and ATCM recommends the tube potential with the lowest radiation dose, estimated on the basis of the patient's topograms, and adjusts the tube current for different patient body habitus during liver CT, consequently leading to an effectively reduced radiation dose while maintaining diagnostic image quality. In

the qualitative analysis of our study, patients showed neither diagnostically unacceptable range of image noise nor unacceptable image quality in groups A1 and A2 in which ATVS and ATCM were simultaneously used. Moreover, with the newly developed ATVS method, at intraindividual analysis we saw a significant percentage decrease in radiation dose of 20% (7.7 mGy \pm 2.2 for AP, 9.4 mGy \pm 1.6 for DP) in group A1 and 31% (6.9 mGy \pm 3.3 for AP, 9.6 mGy \pm 2.3 for DP) in group A2 compared with the results of conventional 120-kV scanning during the DP.

Our results demonstrated that a significant radiation dose reduction was obtained in all patients except the severely obese patients (BMI, >30 kg/

m²). In underweight and normal-weight patients, the radiation dose reduction was greatest as lower tube voltage was selected and used. Severely obese patients, although there were only a small number of patients in our study, required higher tube voltage and radiation dose to obtain a similar image quality. We believe that the combined use of ATVS and ATCM can further increase the range of radiation dose reduction compared with the use of ATCM only, especially in patients with small or regular body habitus (BMI, <23 kg/m²). Considering that tube voltage has an exponential relationship with radiation dose, while radiation exposure is linearly proportional to tube current (8), lowering the tube voltage

Figure 4



Figure 4: Transverse contrast-enhanced (a) AP, (b) PVP, and (c) DP CT images in 48-year-old man (BMI, 28.08 kg/m²) in group B obtained with the use of ATCM alone with a fixed tube potential of 120 kV during all phases. A simple hepatic cyst is seen in segment VII on PVP image (b). Window setting was optimized at a window width of 350 HU and a window level of 40 HU for all images. For AP, PVP, and DP images, CTDI_{vol} was 14.58, 14.42, and 14.30 mGy, while the mean image noise was 11.5, 12.3, and 12.0 HU, respectively, measured at the subcutaneous fat of the anterior abdominal wall.

Table 6

Lesion Conspicuity and Tumor-to-Liver Contrast of 46 Hypervascular Hepatocellular Carcinomas

| Parameter | Group A1 (n = 15) | Group A2 (n = 12) | Group B (n = 19) | Weighted κ | PValue* | PValue† | | |
|------------------------------|-------------------|-------------------|------------------|------------|---------|----------|---------|---------|
| | | | | | | A1 vs A2 | A1 vs B | A2 vs B |
| Tumor-to-liver contrast (HU) | 54.5 ± 6.1 | 59.5 ± 5.0 | 37.5 ± 3.8 | ... | .006 | .28 | <.0001 | <.0001 |
| Lesion conspicuity | 3.3 ± 0.3 | 3.5 ± 0.3 | 3.2 ± 0.2 | 0.68 | .72 | NS | NS | NS |

Note.—Data are means ± standard errors. NS = not significant.

* Calculated by using the Kruskal-Wallis test.

† Calculated by using the Mann-Whitney U test. Bonferroni-corrected P value is .017.

can be a successful way to reduce radiation dose.

Interestingly, there were no cases in which 120 kV was recommended by the ATVS program in our study population. From June to August 2010, there were only two patients for whom 120 kV was recommended by Care kV as the optimal tube potential, both of whom were in group A2. However, even these patients were excluded from our study population because one patient had undergone two-phase abdominal and pelvic CT and the other patient had a different reconstruction algorithm used. The main reasons 120 kV was not selected in groups A1 and A2 were twofold: (a) the issue of tube load and switching tube voltage during the initial phase of the Care kV program and (b) the limited number of patients with a high BMI. First of all, the biggest

reason for the somewhat rare selection of 120 kVp in our study population was that the algorithm for selection of tube potential has a very pure “physics” parameterization in maintaining equal CNR, which may sometimes result in rather nonintuitive behavior (as in the handling of tube voltage switching conflicts). For example, even a relatively small violation of CNR would trigger a switch to 140 kV at the cost of increased dose, rather than sticking to 120 kV with some loss to CNR which would affect image quality minimally but provide lower radiation dose. Therefore, further consideration of correct conflict settings is required with the Care kV system. Second, we believe that the paucity of patients with high BMI in our study group contributed to the even rarer selection of 120 kV in our study. With this small number of

patients with a high BMI, the evaluation of optimal tube potential, especially higher tube voltages of 120 or 140 kV, is inevitably limited.

In our study, the two different ATVS settings used in groups A1 and A2 were intended to provide contrast gains of 1.624 and 1.891, respectively, when going from 140 to 80 kV. Our results demonstrated that the ATVS setting used in group A1 might be preferred for the liver CT protocol to that in group A2 because of the better scores in all of the qualitative analysis criteria, increased CNRs, and less image noise at quantitative analysis. Furthermore, we also found that group A1 showed similar or slightly better overall image quality score than group B, at the price of higher noise. These results could be related to the diagnostic task of the liver CT scan in our study because detection of

hypervascular and/or hypovascular focal liver lesions or demonstration of intrahepatic vessels was of primary importance in most patients (13,29,32,33). The tumor-to-liver contrast in hypervascular hepatocellular carcinomas and the score for visibility of small vasculatures improved with the ATVS setting of group A1 compared with the standard protocol of group B. Moreover, we believe that the ATVS setting used in group A1 might also be effective in the detection of hypovascular hepatic lesions, owing to the improved hepatic parenchymal enhancement compared with group B. However, we did not evaluate whether the combined use of ATVS and ATCM could improve the diagnostic performance of liver CT for detecting hypervascular or hypovascular tumors because we believe that this question would better be answered in a further study.

There were some limitations to our study. First, as stated previously, this study was a retrospective study in a single institution, and we did not directly compare different CT protocols. We had decided not to perform a direct comparison of CT protocols because it would have required the test group to receive a substantially higher radiation exposure than that required for clinical practice, making it ethically untenable. Second, because there were only a small number of patients with hypervascular hepatocellular carcinomas, diagnostic accuracy for lesion detection was not evaluated in this study. However, we did assess lesion conspicuity and tumor-to-liver contrast in patients with hypervascular hepatocellular carcinomas. Finally, there was only a limited number of patients with a BMI greater than 30 kg/m², although this may be unavoidable in Asian countries where severely obese patients are relatively rare. Therefore, application of our study results to Western countries would be rather limited, and additional studies to validate the advantages of the synchronous use of ATVS and ATCM in patients with a BMI greater than 30 kg/m² would be required.

In conclusion, the combined use of ATVS and ATCM for liver CT led to significant radiation dose reduction while

maintaining acceptable image quality through the suggestion of tube voltage and current with the lowest radiation dose, calculated relative to the patient's body habitus, anatomic region being studied, and clinical indications.

Acknowledgments: We thank Bonnie Hami, MA, and Chris Woo, BA, for their editorial assistance and the Medical Research Collaborating Center of Seoul National University Hospital for the statistical advice performed in this study.

Disclosures of Conflicts of Interest: **K.H.L.** No relevant conflicts of interest to disclose. **J.M.L.** Financial activities related to the present article: none to disclose. Financial activities not related to the present article: author receives money as a board member of Bayer Healthcare; author receives grants from Bayer Healthcare and GE Healthcare; author receives payment for lectures from Bayer Healthcare, GE Healthcare, and Siemens Healthcare. Other relationships: none to disclose. **S.K.M.** No relevant conflicts of interest to disclose. **J.H.B.** No relevant conflicts of interest to disclose. **J.H.P.** No relevant conflicts of interest to disclose. **T.G.F.** Financial activities related to the present article: none to disclose. Financial activities not related to the present article: author is employee of Siemens Healthcare. Other relationships: none to disclose. **K.W.K.** No relevant conflicts of interest to disclose. **S.J.K.** No relevant conflicts of interest to disclose. **J.K.H.** No relevant conflicts of interest to disclose. **B.I.C.** No relevant conflicts of interest to disclose.

References

- Baskerville JR. Screening patients with multi-detector computed axial tomography (MDCT): when will we inform patients about the risk of radiation? *Emerg Med J* 2008;25(6):323–324.
- Brenner DJ, Hall EJ. Computed tomography: an increasing source of radiation exposure. *N Engl J Med* 2007;357(22):2277–2284.
- Fazel R, Krumholz HM, Wang Y, et al. Exposure to low-dose ionizing radiation from medical imaging procedures. *N Engl J Med* 2009;361(9):849–857.
- Rizzo S, Kalra M, Schmidt B, et al. Comparison of angular and combined automatic tube current modulation techniques with constant tube current CT of the abdomen and pelvis. *AJR Am J Roentgenol* 2006;186(3):673–679.
- Kalra MK, Rizzo SM, Novelline RA. Reducing radiation dose in emergency computed tomography with automatic exposure control techniques. *Emerg Radiol* 2005;11(5):267–274.
- Mulkens TH, Bellinck P, Baeyaert M, et al. Use of an automatic exposure control mechanism for dose optimization in multi-detector row CT examinations: clinical evaluation. *Radiology* 2005;237(1):213–223.
- McCullough CH, Bruesewitz MR, Kofler JM Jr. CT dose reduction and dose management tools: overview of available options. *RadioGraphics* 2006;26(2):503–512.
- Gunn ML, Kohr JR. State of the art: technologies for computed tomography dose reduction. *Emerg Radiol* 2010;17(3):209–218.
- Haaga JR. Radiation dose management: weighing risk versus benefit. *AJR Am J Roentgenol* 2001;177(2):289–291.
- Kalra MK, Maher MM, Toth TL, et al. Strategies for CT radiation dose optimization. *Radiology* 2004;230(3):619–628.
- McCullough CH, Primak AN, Braun N, Kofler J, Yu L, Christner J. Strategies for reducing radiation dose in CT. *Radiol Clin North Am* 2009;47(1):27–40.
- Yu L, Bruesewitz MR, Thomas KB, Fletcher JG, Kofler JM, McCullough CH. Optimal tube potential for radiation dose reduction in pediatric CT: principles, clinical implementations, and pitfalls. *RadioGraphics* 2011;31(3):835–848.
- Marin D, Nelson RC, Schindera ST, et al. Low-tube-voltage, high-tube-current multidetector abdominal CT: improved image quality and decreased radiation dose with adaptive statistical iterative reconstruction algorithm—initial clinical experience. *Radiology* 2010;254(1):145–153.
- Yu L, Li H, Fletcher JG, McCullough CH. Automatic selection of tube potential for radiation dose reduction in CT: a general strategy. *Med Phys* 2010;37(1):234–243.
- Singh S, Kalra MK, Moore MA, et al. Dose reduction and compliance with pediatric CT protocols adapted to patient size, clinical indication, and number of prior studies. *Radiology* 2009;252(1):200–208.
- Rapalino O, Kamalian S, Kamalian S, et al. Cranial CT with adaptive statistical iterative reconstruction: improved image quality with concomitant radiation dose reduction. *AJNR Am J Neuroradiol* 2012;33(4):609–615.
- Kambadakone AR, Chaudhary NA, Desai GS, Nguyen DD, Kulkarni NM, Sahani DV. Low-dose MDCT and CT enterography of patients with Crohn disease: feasibility of adaptive statistical iterative reconstruction. *AJR Am J Roentgenol* 2011;196(6):W743–W752.
- Vorona GA, Ceschin RC, Clayton BL, Sutcliffe T, Tadros SS, Panigrahy A. Reducing abdominal CT radiation dose with the adaptive statistical iterative reconstruction tech-

- nique in children: a feasibility study. *Pediatr Radiol* 2011;41(9):1174–1182.
19. Kalender WA, Deak P, Kellermeier M, van Straten M, Vollmar SV. Application- and patient size-dependent optimization of x-ray spectra for CT. *Med Phys* 2009;36(3):993–1007.
 20. Nakayama Y, Awai K, Funama Y, et al. Abdominal CT with low tube voltage: preliminary observations about radiation dose, contrast enhancement, image quality, and noise. *Radiology* 2005;237(3):945–951.
 21. Schindera ST, Nelson RC, Mukundan S Jr, et al. Hypervascular liver tumors: low tube voltage, high tube current multi-detector row CT for enhanced detection—phantom study. *Radiology* 2008;246(1):125–132.
 22. Utsunomiya D, Oda S, Funama Y, et al. Comparison of standard- and low-tube voltage MDCT angiography in patients with peripheral arterial disease. *Eur Radiol* 2010;20(11):2758–2765.
 23. Winklehner A, Goetti R, Baumüller S, et al. Automated attenuation-based tube potential selection for thoracoabdominal computed tomography angiography: improved dose effectiveness. *Invest Radiol* 2011;46(12):767–773.
 24. Shiwaku K, Anuurad E, Enkhmaa B, Kitajima K, Yamane Y. Appropriate BMI for Asian populations. *Lancet* 2004;363(9414):1077.
 25. Awai K, Takada K, Onishi H, Hori S. Aortic and hepatic enhancement and tumor-to-liver contrast: analysis of the effect of different concentrations of contrast material at multi-detector row helical CT. *Radiology* 2002;224(3):757–763.
 26. Spielmann AL, Nelson RC, Lowry CR, et al. Liver: single breath-hold dynamic subtraction CT with multi-detector row helical technology feasibility study. *Radiology* 2002;222(1):278–283.
 27. Kalra MK, Maher MM, Blake MA, et al. Detection and characterization of lesions on low-radiation-dose abdominal CT images postprocessed with noise reduction filters. *Radiology* 2004;232(3):791–797.
 28. Bruix J, Sherman M; American Association for the Study of Liver Diseases. Management of hepatocellular carcinoma: an update. *Hepatology* 2011;53(3):1020–1022.
 29. Marin D, Nelson RC, Samei E, et al. Hypervascular liver tumors: low tube voltage, high tube current multidetector CT during late hepatic arterial phase for detection—initial clinical experience. *Radiology* 2009;251(3):771–779.
 30. Nakaura T, Awai K, Oda S, et al. Low-kilovoltage, high-tube-current MDCT of liver in thin adults: pilot study evaluating radiation dose, image quality, and display settings. *AJR Am J Roentgenol* 2011;196(6):1332–1338.
 31. Hausleiter J, Martinoff S, Hadamitzky M, et al. Image quality and radiation exposure with a low tube voltage protocol for coronary CT angiography results of the PROTECTION II Trial. *JACC Cardiovasc Imaging* 2010;3(11):1113–1123.
 32. Marin D, Nelson RC, Barnhart H, et al. Detection of pancreatic tumors, image quality, and radiation dose during the pancreatic parenchymal phase: effect of a low-tube-voltage, high-tube-current CT technique—preliminary results. *Radiology* 2010;256(2):450–459.
 33. Robinson E, Babb J, Chandarana H, Macari M. Dual source dual energy MDCT: comparison of 80 kVp and weighted average 120 kVp data for conspicuity of hypovascular liver metastases. *Invest Radiol* 2010;45(7):413–418.